Analysis of a multitrait population projection matrix reveals the evolutionary and demographic effects of a life history trade-off

Christophe F.D. Coste, Samuel Pavard

Analysis of a multitrait population projection matrix reveals the evolutionary and demographic effects of a life history trade-off

Christophe F. D. Coste[1,2] and Samuel Pavard[2]

[1]Centre for Biodiversity Dynamics, Department of Biology, Norwegian University of Science and Technology, Trondheim, Norway
[2]Unité Eco-anthropologie (EA), Muséum National d'Histoire Naturelle, CNRS, Université Paris Diderot, F-75016, Paris, France

Abstract

It is increasingly recognized that incorporating life history trade-offs into evolutionary demography models requires trade-offs to be decomposed into *fixed* (a.k.a *genetic*) and *individual* (a.k.a *dynamic*) components. This is fundamental in order to understand how trade-offs are related to *fixed* and *dynamic* components of individual heterogeneities and generate variance in individual trajectories. Therefore, embedding such trade-offs into population projection matrices usually requires three categories: a *life-history determining* trait (e.g., age or stage), a *fixed* trait incorporating the *genetic* trade-off, and a *dynamic* trait modeling the *individual* component. This has proved a complex exercise until the recent advent of *Multitrait Population Projection Matrices* (MPPMs)[1]. Recent developments of *Trait-Level Analysis* (TLA)[2] tools for MPPMs now allow us to study the demographic and evolutionary consequences of each component of a life history trade-off. Here, we illustrate this by constructing and analyzing an evolutionary demography model that implements both *dynamic* and *fixed* components of the *costs of reproduction*, the trade-off between current/early reproduction and future/later fitness. In particular, we explain and describe the use of the TLA to measure the effects of this trade-off on individual fitness. Here, we focus on the variance of lifetime reproductive success between models implementing the *individual* costs and asymptotically-equivalent matrices from which they are absent. This allows us to show that *dynamic* costs decrease that variance and more so for slow organisms. Therefore, accounting for this component of the costs, instead of classically focusing solely on *fixed* costs of reproduction, is paramount in order to correctly assess the relative importance of the "neutral" and "adaptive" components of individual heterogeneity.

Keywords: Trait level analysis; Life history theory; Life-history trade-offs; Multitrait population projection matrices; Evolutionary demography; Individual heterogeneity; Hyperstate matrix models.

Highlights:

- A novel typology of life history trade-offs is proposed

- Multitrait matrices allow to incorporate fixed and dynamic components of trade-offs

- Effects of trade-offs on population dynamics are analyzed via Trait Level Analysis

- Individual costs of reproduction decrease variance in Lifetime Reproductive Success

- Individual costs of reproduction reduce relative importance of "neutral" individual heterogeneity

---

[1]MPPM: Multitrait (i.e., multi-category) Population Projection Matrix
[2]TLA: Trait Level Analysis, a toolbox for MPPMs developed by Coste et al. (2017)

1 Introduction

Trade-offs are at the core of life history theory. They occur "when an increase in fitness due to a change in one trait is opposed by a decrease in fitness due to a concomitant change in the second trait" (Roff and Fairbairn, 2007, p.433). These *Life History Trade-Offs* (LHTOs)[1]s – without which nature would be filled with "Darwinian demons" (Law, 1979) – are deemed ubiquitous. They are studied by the various fields of evolutionary biology that make up life history theory and in particular three of them. In quantitative genetics, they are a major component of the **G** matrix (Lande, 1982). Physiologists focus on the mechanistic constraints, mainly homeostatic, yielding trade-offs (for instance because of a Y-shaped allocation of finite resources; Orton, 1929; Lack, 1954; Cody, 1966). Behavioral ecologists study environmentally-mediated trade-offs (e.g., Jessup and Bohannan, 2008). Paradoxically however, LHTOs have rarely been implemented into Evolutionary Demography models. This can be due to technical difficulties in doing so, or because population and individual mechanisms are studied by different families of models while trade-offs act at both these levels (see appendix A).

However, this shortcoming is most likely caused by demographers' early realization that the classical classification of LHTOs into physiological, behavioral and genetic trade-offs (see appendix B) lacks clarification pertaining to conceptual differences, overlaps or equivalences between these three families (as discussed in Stearns, 1992; Roff, 1993).

To be implementable into evolutionary demography models, trade-offs require a novel typology that provides a proper demographic *decomposition* instead of a mechanistic *classification*. We argue that this can be achieved by projecting, onto the field of Population Projection Matrices (PPMs), the decomposition of individual heterogeneity into *fixed* and *dynamic* components devised by Tuljapurkar, Steiner and Orzack (Tuljapurkar et al., 2009; Steiner et al., 2010; Tuljapurkar and Steiner, 2010); itself leading to the decomposition of demographic traits (a.k.a. categories) into *static* and *dynamic* classes (Vindenes and Langangen, 2015). Instead of merely *classifying* trade-offs according to the assumed locations of their constraint mechanisms, this novel typology of trade-offs *decomposes* LHTOs into two components with respect to the means by which they affect phenotypic variance.

The first component is the *fixed-at-birth* component (a.k.a *genetic*, *fixed* or *static*). It can be heritable because some of the phenotypic variance stems from genetic variance, because of shared parent-offspring environments or because of epigenetics. In this paper, for simplification, we focus on *fixed* components of LHTOs, which are genetically fixed. However the concepts and the model can be extended to incorporate other forms of fixed-trait heritability. When applied to trade-offs, such a *genetic* component of a LHTO (or simply *genetic* LHTO) generates a gradient of coexisting *strategies* in the population: some "lineages" having a constantly better trait A and a worse trait B than others. The second component is the *individual* component (a.k.a. *dynamic*). *Individual* LHTOs encompass the "mechanistic", internal or external, individual constraints that organisms have to deal with at every timestep of their lives (when, for instance, allocating a limited amount of energy between two traits within a particular environment). *Individual* LHTOs yield different possible realizations of each of the aforementioned strategies, via their interaction with individual stochasticity. In other words, individuals of the same, genetically-determined life-history *strategy* may experience different life-history *trajectories* due to "luck" (Caswell, 2009; Tuljapurkar et al., 2009; Snyder and Ellner, 2018). Therefore, using the current nomenclature (see Steiner and Tuljapurkar, 2012; Cam et al., 2016; Hamel et al., 2018), we can write that the *fixed* component of trade-offs generates "adaptive" heterogeneity and the *individual* component controls "neutral" heterogeneity. The decomposition of a trade-off into *fixed* and *individual* components is additive and can therefore be implemented into PPMs. We argue that such an implementation would benefit life history theory and evolutionary demography. It would, for instance, enable measuring the evolutionary importance of the *individual* component of LHTOs, which is usually considered to have no evolutionary effects, as their demographic consequences "average out" in large populations (Snyder and Ellner, 2018).

Here, we implement both *genetic* and *individual* components of the *Costs of Reproduction* (CoR)[2], the "most prominent of all trade-offs" according to Stearns (1989) as it directly relates the two highest-level components of fitness. CoR is the trade-off between current/early reproduction and future/later fitness (i.e., future/later survival and reproduction). The *genetic* component of such a trade-off consists of the intraspecific gradient in strategies along the slow–fast continuum. Slower lineages promote higher survival (and therefore longevity) at the cost of fertility compared to faster lineages. The *individual* component of the CoR reduces the vital rates of individuals as they exert reproductive efforts. However, since re-

---

[1]LHTO: Life History Trade-off
[2]CoR: Costs of Reproduction

productive and survival events are subject to individual stochasticity (i.e., to chance), the realization of this trade-off over the several timesteps of an individual life trajectory follows itself a stochastic process. Indeed, two individuals sharing the same (*genetic/fixed*) strategy may end up with very different trajectories as individual stochasticity in reproductive realizations generate deviations from the central strategy evolved by the lineage.

In order to incorporate both *genetic* and *individual* components of the CoR into a PPM, we build a three-trait MPPM. Indeed incorporating trade-offs requires at least three traits: the "usual" *life-history determining* trait (e.g. *age*, *size*, or *stage*), a *fixed* trait embedding the *genetic* trade-off, and a *dynamic* trait incorporating the *individual* component. The construction of such MPPMs has recently been streamlined (Roth and Caswell, 2016; Coste et al., 2017). Moreover, a new analytical tool, the Trait Level Analysis (TLA, see Coste et al., 2017)) now allows us to analyze the demographic and evolutionary importance of each trait in an MPPM (Coste et al., 2017). Applied to a model implementing trade-offs, the TLA makes it possible to measure the evolutionary consequences of the *fixed* and the *individual* components of a LHTO. Here, to investigate the CoR, we use a very common *life-history determining* trait in the literature of demographic models: *age*. Incorporating the *individual* component of the costs requires a trait that accounts for the accumulated reproductive efforts of individuals; we use *parity* which tracks the number of offspring ever born. In order to implement the *fixed* component of the costs, we introduce a trait *strategy* that positions a lineage along the intraspecific slow–fast continuum (the parent's strategy being possibly inherited by its daughter). We therefore construct an (*age-parity-strategy*) MPPM projecting over time a population encountering both fixed and individual CoR. This three-trait MPPM is then analyzed via the TLA in order to disentangle the evolutionary and demographic effects of each component. The MPPM is considered in a general form, however the tools presented can readily be applied for a model built from empirical data (see appendix C). For illustrative and practical purposes we reduce the number of degrees of freedom to the fewest possible, but such a model can also be built with numerous *fixed* and *individual* components.

This model is obviously too simple to be a proper population genetics model, as this would also require the incorporation of new alleles generated via molecular mutations and of diploidy (i.e., be a two-sex model). Both limitations are common in extensions of projection models towards population genetics (see, e.g., de Vries and Caswell, 2019). Moreover, this model cannot be considered a quantitative genetics one, as this would require the ability to incorporate a continuous trait space. However, turning the MPPM into an integral population model (Rees et al., 2014), would allow the model to be extended from discrete to continuous trait values. It is however not the aim of this article to develop a (population or quantitative) genetics model, but to show how the addition of carefully chosen traits onto a demographic model can yield, via the TLA, invaluable information about the evolutionary importance of the studied trade-offs.

To perform such an analysis, we focus on a key fitness measure: lifetime reproductive success $\mathcal{LRS}$, considered as a random variable. It measures the number of offspring produced by an individual in the population during its lifetime. The expectation of $\mathcal{LRS}$ is the much used *net reproductive rate* $\mathcal{R}_0$; the variance of $\mathcal{LRS}$ is denoted $\sigma^2_{\mathcal{LRS}}$. Whereas the growth rate λ is often used as a genotype or population measure of fitness (either as λ_1, the dominant eigenvalue, for deterministic models or as λ_s, the stochastic growth rate, for models incorporating environmental or demographic variance), $\mathcal{LRS}$ is an individual measure. Many authors consider it a less relevant fitness measure than λ at the population level because it does not account for life pacing and reproductive rhythm (Nur, 1984; Murray, 1992; Giske et al., 1993). Indeed, $\mathcal{LRS}$ loses track of chronological time – a major shortcoming for models with overlapping generations. However, it has the advantage of being an individual measure, readily aggregated at the population level. This is not the case for λ, despite efforts to conceive an "individual growth rate" however still difficult to fathom (McGraw and Caswell, 1997). Initial results stemming from the application of TLA to CoR are already known (see for instance the reducing effects of individual CoR on selection gradients in Coste et al., 2017), but most still remain to be investigated. Here, we focus on the effects of the *individual* component of costs on $\sigma^2_{\mathcal{LRS}}$ by comparing models implementing this trade-off and asymptotically-equivalent matrices from which it is absent (via an operation called *folding*; see Coste et al., 2017). We analyze how these effects depend on the position of species/lineages on the slow–fast continuum generated by *genetic* CoR. In particular, we will show that *individual* CoR decrease the variance in reproductive success and do so more strongly in slow organisms than fast ones. We will also show that neglecting *individual* costs and focusing solely on *fixed* costs, which is a common practice in evolutionary demography, can yield to overestimating the "neutral" component of fixed heterogeneity at the expense of the "adaptive" one.

2 Materials and Methods

2.1 Theoretical MPPM for both components of CoR

In order to disentangle the effects of *individual* and *fixed* components of costs, the vital rates (i.e., fertility and survival rates) are decomposed into two independent components. First, the *strategy* is modeled by the *zero-parity* vital rates (the vital rates of individuals which have yet to reproduce). A slower strategy will have lower zero-parity fertility but higher zero-parity survival rates than a faster one, but both lineages may have the same fitness (the same growth rate). At the population level, this spectrum of strategies constitutes the *fixed* component of CoR. Second, these zero-parity vital rates are then linearly reduced with increased parity, possibly down to zero. This parity effect models the *individual* components of CoR, since the changes in parity value is a stochastic process that depends on reproductive history and demographic stochasticity.

Thus, the vital rates $vr_{a,p,st}$ (vr being either a survival or fertility rate) of an individual of age a, parity p and strategy st are provided by the following formula:

$$vr_{a,p,st} = \underbrace{\left(1 - \frac{p}{\beta - \alpha + 1}\right)}_{\text{parity effect} \rightarrow \textbf{individual component of costs}} \times \underbrace{vr_{a,0,st}}_{\text{zero-parity vital rates} \rightarrow \textbf{genetic component of costs}} \quad , \ (1)$$

where α and β are the ages at first and last reproduction and, for parsimony, zero-parity vital rates are independent of age a and therefore only dependent on strategy st. As an individual of a fast *strategy* (with large zero-parity-fertility rates) is expected to encounter high reproductive success early in adult life, it will have, on average, lower fertility rates late in life than an individual of a slower *strategy* that will have had fewer offspring at that point. However, it is possible in this model to consider an individual of a fast *strategy* but limited reproductive success – because of (bad) luck – that will have higher fertility rates late in life than a very (and unexpectedly) successful slow individual. Since the model incorporates several *strategies*, we have to define a generation transmission parameter. For the purpose of illustration, we therefore incorporate parameter μ that represents the probability for an offspring to be of a different *strategy* than its parent. When only two strategies are considered, we have $0 \leq \mu \leq 0.5$ and this generates a scenario where differing for its parent's strategy can only mean switching from one to the other (a quite unrealistic scenario from a population genetics standpoint). In that case, if $\mu = 0.5$, strategies are randomly distributed at birth (i.e., the strategy is not heritable).

We denote $\mathbf{L}$ this generic formal (*age-parity-strategy*) MPPM. In Expression (2), we illustrate a particular $\mathbf{L}$ for an organism with maximum age $\omega = 3$ years, age at first reproduction $\alpha = 2$ years and age at last reproduction $\beta = 3$ years, with a slow lineage (left half of the matrix, in blue; colours are added for clarity in the online version) with zero-parity vital rates S and f and a fast lineage (right half of the matrix, in red) with zero-parity vital rates s and F (with $s < S$ and $F > f$). Parity can be 0 or 1; there are actually two possible fertility events in every life trajectory but, here, individuals of parity 2 have an abundance of zero, as they have reached maximum lifespan, and are therefore not accounted for. Having parity of 1 divides individual fertility by a factor of 2 compared to having a parity of 0.

In an MPPM, the state of an individual depends on its "position" according to several trait/category axes. This state of an individual, or individual state, corresponds to the i-state of Metz and Diekmann (1986) and, from now on, we shall refer to it, simply, as state. These states form a space, the space of states or state space (which is a product space). The order in which traits are nested in the space of states is crucial to its construction and analysis; its knowledge is required in order to generate the *trait structure* (as per Coste et al., 2017). Here, the space of states is three-dimensional and trait *age* is nested into trait *parity*, and both into trait *strategy*. Formally, it means that the ith element of abundance vector $\boldsymbol{n}$, which matrix $\mathbf{L}$ projects over time, represents the abundances of individuals of age a, parity p, and strategy st, for which $(a + \omega \times p + \omega \times par \times st) = i$, with par the number of parity classes (which can be calculated as $par = min(\beta - \alpha + 2, \omega - \alpha + 1)$). Each (a, p, st) combination corresponds to one and only one position $1 \leq i \leq (\omega \times par \times 2)$ in $\boldsymbol{n}$, and each of these $1 \leq i \leq (\omega \times par \times 2)$ indices corresponds to one and only one (a, p, st) triplet. Here, this means that the state corresponding to trait triplet (a, p, st) will occupy position $a + 3 \times p + 6 \times st$ in the space of individual states (we equate $st = 0$ with the slow strategy and $st = 1$ with the fast one). For instance, this means that individuals of age 2, parity 0 and fast strategy will occupy position 8 in $\boldsymbol{n}$. Abundance vector $\boldsymbol{n}$ is of length $\omega \times par \times 2$, i.e., here, $3 \times 2 \times 2 = 12$ and $\mathbf{L}$ of size 12×12. Vital rates for parities of 1 are represented in lighter shades than the zero-parity rates, such that $\mathbf{L}$ can be written as:

$$\mathbf{L} = \left[\begin{array}{ccccc:cccccc}
\cdot & (1-\mu)F & (1-\mu)F & \cdot & \cdot & (1-\mu)\frac{F}{2} & \cdot & \mu f & \mu f & \cdot & \cdot & \mu\frac{f}{2} \\
s & \cdot & \cdot & \cdot & \cdot & \cdot & \cdot & \cdot & \cdot & \cdot & \cdot & \cdot \\
\cdot & s(1-F) & \cdot & \cdot & \cdot & \cdot & \cdot & \cdot & \cdot & \cdot & \cdot & \cdot \\
\cdot & \cdot & \cdot & \cdot & \cdot & \cdot & \cdot & \cdot & \cdot & \cdot & \cdot & \cdot \\
\cdot & sF & \cdot & \cdot & \cdot & \cdot & \cdot & \cdot & \cdot & \cdot & \cdot & \cdot \\
\hdashline
\cdot & \mu F & \mu F & \cdot & \cdot & \mu\frac{F}{2} & \cdot & (1-\mu)f & (1-\mu)f & \cdot & \cdot & (1-\mu)\frac{f}{2} \\
\cdot & \cdot & \cdot & \cdot & \cdot & \cdot & S & \cdot & \cdot & \cdot & \cdot & \cdot \\
\cdot & \cdot & \cdot & \cdot & \cdot & \cdot & \cdot & S(1-f) & \cdot & \cdot & \cdot & \cdot \\
\cdot & \cdot & \cdot & \cdot & \cdot & \cdot & \cdot & \cdot & \cdot & \cdot & \cdot & \cdot \\
\cdot & \cdot & \cdot & \cdot & \cdot & \cdot & \cdot & Sf & \cdot & \cdot & \cdot & \cdot \\
\end{array} \right]. \quad (2)$$

2.2 *Folding* the (*age-parity-strategy*) MPPM

The TLA of an MPPM aims at understanding the demographic and evolutionary importance of traits for the dynamics of a population (Coste et al., 2017). It is the trait counterpart of the classical sensitivity/elasticity analysis to matrix entries (Goodman, 1971; Caswell, 1978; de Kroon et al., 1986). In order to measure the sensitivity of fitness values (or any other asymptotic measure) to traits, the TLA asks how these values are affected by the *folding* of the matrix over one or several of its categories (a.k.a. traits). *Folding*, as detailed by Coste et al. (2017), consists in *merging* states (i.e., combinations of traits or matrix entries) sharing the same values for the traits to be *folded* upon, in a manner that preserves the asymptotic flows of individuals between those states. Simply put, Ergodic-Flow-Preserving-*merging* of matrix entries consists in summing the outgoing transitions and averaging the incoming ones weighted by asymptotic abundances. This approach has been theorized by Enright et al. (1995), Hooley (2000) and Salguero-Gómez and Plotkin (2010). *Folding*, at the core of the TLA, extends the operation of EFP-*merging* from states to traits.

In the case of MPPM **L** incorporating the traits *parity* and *strategy*, successive *foldings* over these traits provide information on the respective consequences of the *individual* and *genetic* components of CoR. We hereafter denote $\mathbf{L}^{\text{fold}}_{\text{age,parity}}$, $\mathbf{L}^{\text{fold}}_{\text{age,strategy}}$, and $\mathbf{L}^{\text{fold}}_{\text{age}}$ the matrix **L** respectively *folded* over *strategy*, over *parity*, and over both. Matrix $\mathbf{L}^{\text{fold}}_{\text{age}}$ is also called the *Reference Leslie Matrix*, and its comparison with **L** provides information regarding the evolutionary importance of both – *individual* and *genetic* – components of the CoR.

As an illustration of the *folding* mechanism, from the formal 3-year model described above (in Expression (2), with $\alpha = 2$, $\beta = 3$ and 2 *strategies*), we draw a specific model **L1** with two iso-fitness genotypes of asymptotic growth rate $\lambda \approx \mathcal{R}_0 \approx 1$ (we denote λ here the dominant eigenvalue of the deterministic matrix). In this case, vital rates are $F = 0.95$ and $s = 0.7541$ for the fast strategy, and $f = 0.7013$ and $S = 0.9$ for the slow strategy. Reproduction is considered as a random process constituted of Bernoulli independent trials (one offspring maximum, per timestep). The transmission parameter is $\mu = 0.25$. We get (all transition probabilities between individual states are rounded off to the nearest ten thousandth):

$$\mathbf{L1} = \left[\begin{array}{ccccc:cccccc}
\cdot & 0.7125 & 0.7125 & \cdot & \cdot & 0.3563 & \cdot & 0.1753 & 0.1753 & \cdot & \cdot & 0.0877 \\
0.7541 & \cdot & \cdot & \cdot & \cdot & \cdot & \cdot & \cdot & \cdot & \cdot & \cdot & \cdot \\
\cdot & 0.0377 & \cdot & \cdot & \cdot & \cdot & \cdot & \cdot & \cdot & \cdot & \cdot & \cdot \\
\cdot & \cdot & \cdot & \cdot & \cdot & \cdot & \cdot & \cdot & \cdot & \cdot & \cdot & \cdot \\
\cdot & 0.7164 & \cdot & \cdot & \cdot & \cdot & \cdot & \cdot & \cdot & \cdot & \cdot & \cdot \\
\hdashline
\cdot & 0.2375 & 0.2375 & \cdot & \cdot & 0.1188 & \cdot & 0.5260 & 0.5260 & \cdot & \cdot & 0.2630 \\
\cdot & \cdot & \cdot & \cdot & \cdot & \cdot & 0.9 & \cdot & \cdot & \cdot & \cdot & \cdot \\
\cdot & \cdot & \cdot & \cdot & \cdot & \cdot & \cdot & 0.2688 & \cdot & \cdot & \cdot & \cdot \\
\cdot & \cdot & \cdot & \cdot & \cdot & \cdot & \cdot & \cdot & \cdot & \cdot & \cdot & \cdot \\
\cdot & \cdot & \cdot & \cdot & \cdot & \cdot & \cdot & 0.6312 & \cdot & \cdot & \cdot & \cdot \\
\end{array} \right]. \quad (3)$$

Its normalized right eigenvector $\mathbf{w(L1)} = [19.87 \ 15.00 \ 0.57 \ 0 \ 0 \ 10.75 \ 19.87 \ 17.87 \ 4.78 \ 0 \ 0 \ 11.29]^{\mathsf{T}}\%$ (where each entry is rounded off to the nearest hundredth) can be written in 3-dimensional form as:

		strategy					
		age	19.87%	17.87%	4.78%		
			0.00%	0.00%	11.29%		
parity	19.87%	15.00%	0.57%				
	0.00%	0.00%	10.75%				

From the latter, we can construct the weight matrices $\mathbf{Wght}$ and, from the characteristics of the traits to be folded upon (the "trait structure"), one can generate the Block-Folding permutation matrices $\mathbf{P^{BF}}$ which, together, generate the folding matrices as per Eq.(4) from Coste et al. (2017). This yields $\mathbf{L1^{fold}_{age,strategy}}$ (i.e., $\mathbf{L1}$ *folded* over trait *parity*): a population model where both *fixed* and *individual* components of the costs were initially accounted for, but where *individual* costs are no longer implemented:

$$\mathbf{L1^{fold}_{age,strategy}} = \left[\begin{array}{ccc|ccc} . & 0.7125 & 0.3741 & . & 0.1753 & 0.1138 \\ 0.7541 & . & . & . & . & . \\ . & 0.7541 & . & . & . & . \\ \hline . & 0.2375 & 0.1247 & . & 0.5260 & 0.3415 \\ . & . & . & 0.9 & . & . \\ . & . & . & . & 0.9 & . \end{array} \right]. \tag{4}$$

Calculation-wise, in the particular case of this illustration, the fertility rate for 3-year-old, slow individuals in $\mathbf{L1^{fold}_{age,strategy}}$, 0.3741, can be easily obtained by averaging the corresponding fertility rates in $\mathbf{L1}$ (0.7125 for the individuals of *parity* 0 and 0.3563 for the individuals of *parity* 1) with weights corresponding to the relative abundances of these two states: ($\frac{0.57\%}{0.57\%+10.75\%}$ for the individuals of *parity* 0 and $\frac{10.75\%}{0.57\%+10.75\%}$ for the individuals of *parity* 1).

Matrix $\mathbf{L1^{fold}_{age}}$ is the Reference Leslie Matrix obtained by *folding* $\mathbf{L1}$ over the *parity* and *strategy* traits (a PPM where CoR are accounted for but *not* implemented):

$$\mathbf{L1^{fold}_{age}} = \left[\begin{array}{ccc} . & 0.8147 & 0.4733 \\ 0.8271 & . & . \\ . & 0.8335 & . \end{array} \right]. \tag{5}$$

Vital rates are an *input* of the initial matrix $\mathbf{L1}$ embedding CoR (as for classical matrix models). However, they are an *output* of the *folded* models For these *folded* models, the *induced* vital rates can be gathered directly, or computed, from the entries of the matrices. In our illustration, vital rates for the Reference Leslie Matrix $\mathbf{L1^{fold}_{age}}$ are readily readable, in Eq. (5), on the first line (fertility rates) and the subdiagonal (survival rates). Each of the two block-matrices (one for each *strategy*) of $\mathbf{L^{fold}_{age,strategy}}$ can also be treated as such (Eq. 4). With regards to $\mathbf{L^{fold}_{age,parity}}$, calculations are similar: fertilities are to be found on the first line and the other entries sum up column-wise to the survival rates; note, however, that the interpretation of $\mathbf{L^{fold}_{age,parity}}$ (and for that matter of any multitrait model *folded* over one of its *dynamic* trait) is to be treated with care (see Supplementary Material S.1).

By construction, λ is preserved by *folding*, but what about $\mathcal{R}_0$? In the general case, this is not true (see Supplementary Material S.2). In the particular case of MPPMs with trait *age*, however, $\mathcal{R}_0$ is preserved by *folding* (proof in Supplementary Material S.3; note that, as PPMs project populations over time, it is always possible to incorporate *age* as a trait). Therefore, as for λ, the effects of LHTOs on $\mathcal{R}_0$ will be measured by their consequences on the higher moments of $\mathcal{LRS}$ and chiefly its variance $\sigma^2_{\mathcal{LRS}}$.

2.3 Variance in Reproductive Success for MPPMs

For MPPMs with both *dynamic* and *fixed* traits, the calculation of $\sigma^2_{\mathcal{LRS}}$ requires the use of a tool for which the fertility processes are not formalized as *vectors* of moments per input state i, but as a *matrix* containing the different moments of fertility for an individual surviving from state i to state j. A Markov chain with rewards (MCwR) is such a tool, where the "reward" matrix can implement the various moments of $\mathcal{F}$, the fertility stochastic process, as a function of both ends of an $i \to j$ transition. We will thus use MCwRs to compute variance $\sigma^2_{\mathcal{LRS}}$ for the(*age-parity-strategy*) MPPM $\mathbf{L}$.

To describe the MCwR mathematical framework, introduced by Howard (1960) and Hatori (1966), we will use the approach of Caswell (2011), who was the first to have applied this tool to demography. The MCwR framework requires two instruments. First, $\tilde{\mathbf{T}}$ which is $\mathbf{T}$ of size $q \times q$ (where q is the number of

states), the usual survival transition matrix, upon which absorbing state *death* is explicitly added in the $q+1^{\text{th}}$ position of the matrix: $\tilde{\mathbf{T}} = \begin{bmatrix} \mathbf{T} & 0 \\ \mathbf{m} & 1 \end{bmatrix}$ ($\mathbf{m}$ is the vector of mortality rates i.e., $\mathbf{m} = \mathbf{1}' - \mathbf{1}'\mathbf{T}$, where $\mathbf{1}$ denotes the q-dimensional vector of ones). Matrix $\tilde{\mathbf{T}}$ is a *stochastic matrix* (columns sum to 1) that fully describes the Markov chain of all possible survival trajectories that any individual in the population can follow before being absorbed by *death*. Second, the family of "reward matrices" $\mathbf{Rw^k}$, where $\mathrm{Rw^k}_{ij}$ is the kth moment of the random variable of the reward (i.e., here, the birth of 1 offspring) for an individual transitioning from state j to state i. Whenever no trade-off involving fertility is involved, matrices $\mathbf{Rw}^k$ have rank 1, with all lines equal to the fertility rate vector. In $\mathbf{L}$ however, current reproductive success does not only depend on the state $i = (a, p, st)$ of the individual, but also on the state j it is transitioning toward. In detail, if $j = (a+1, p+1, st)$, then reproduction is being successful as parity is increased by one unit, and thus its expectation is $\mathrm{Rw}^1_{j,i} = 1$. If $j = (a+1, p, st)$, the individual survives but does not reproduce at that timestep, then $\mathrm{Rw}^1_{j,i} = 0$. Finally, if $j = death$, the individual dies at the end of the period. Then, because fertility and survival processes are independent of their respective realizations (they are not independent per se, as their probability rates depend on their states, which are equal), $\mathrm{Rw}^1_{death,i} = f_i$. This completes the construction of the "reward matrix" $\mathbf{Rw}^1$. It is therefore a zero matrix with the exception of its sub-diagonal, made of 0s, its lower sub-diagonal, made of 1s, and its bottom row corresponding to fertility rates. Because the reproductive rewards are the outcome of Bernoulli independent trials (either 0 or 1 offspring) in our particular illustration, reward matrices for any moment, $\mathbf{Rw}^k$, are equal to the reward matrix of means $\mathbf{Rw}^1$.

Let $\boldsymbol{\rho_k}$ be the vector of the kth moment of $\mathcal{LRS}$, indexed on individuals "starting" states. These are calculated as the convergence of backwards accumulation of "remaining" rewards following individuals from *death* (where no remaining reward remains) to birth (or age $a = 1$). From Caswell et al. (2011), we draw the following convergence equations, for the first two moments:

$$\boldsymbol{\rho_1} = \lim_{t \to \infty} \boldsymbol{\rho_1}(t) \text{ with } \boldsymbol{\rho_1}(t+1) = (\tilde{\mathbf{T}} \circ \mathbf{Rw^1})'\mathbf{1} + \tilde{\mathbf{T}}\boldsymbol{\rho_1}(t), \tag{6}$$

$$\boldsymbol{\rho_2} = \lim_{t \to \infty} \boldsymbol{\rho_2}(t), \text{ with } \boldsymbol{\rho_2}(t+1) = (\tilde{\mathbf{T}} \circ \mathbf{Rw^2})'\mathbf{1} + 2(\tilde{\mathbf{T}} \circ \mathbf{Rw^1})'\boldsymbol{\rho_1}(t) + \tilde{\mathbf{T}}\boldsymbol{\rho_2}(t), \tag{7}$$

and with initial conditions $\boldsymbol{\rho_1}(0) = \boldsymbol{\rho_2}(0) = \mathbf{0}$ ($\circ$ is the Hadamard or elementwise product).

Let us now reduce all $\mathcal{LRS}$ moments $\boldsymbol{\rho_k}$ to states of age $a = 1$ (and thus $p = 0$), i.e., to the offspring states. Then $\boldsymbol{\rho_1}$ and $\boldsymbol{\rho_2}$ are of size the number of classes of trait *strategy*. Then the vectors of expectancy and of variance of $\mathcal{LRS}$ for each offspring class are:

$$\mathbf{e}_{\mathcal{LRS}} = \boldsymbol{\rho_1}, \tag{8}$$

$$\boldsymbol{\sigma}^2_{\mathcal{LRS}} = \boldsymbol{\rho_2} - \boldsymbol{\rho_1} \circ \boldsymbol{\rho_1}. \tag{9}$$

3 Results: Effects of *individual* costs on $\sigma^2_{\mathcal{LRS}}$

We aim at measuring some of the effects of the CoR on $\sigma^2_{\mathcal{LRS}}$, the variance in lifetime reproductive success. Specifically, we focus on comparing the variance of $\mathcal{LRS}$ between models implementing the *individual* costs and asymptotically-equivalent matrices from which they are absent (i.e., *folded* over *parity*). To be able to provide such results, we have constructed MPPMs that incorporate the *individual* and/or the *genetic* component(s) of CoR via the traits *parity* and *strategy*. In the following sections, we first investigate the overall effect of *individual* costs on $\sigma^2_{\mathcal{LRS}}$. Second, we compare the strength of this effect along the gradient of *genetic* costs to determine whether the position of a lineage on the slow–fast continuum has an effect on the strength of *individual* costs on individual fitness. Finally, we investigate the consequences of these results for the relative importance of "adaptive" and "neutral" components of individual heterogeneity.

3.1 *Individual* costs reduce the variance in lifetime reproductive success

In Supplementary Material section S.4, we formally demonstrate (Eq. 18) that *individual* CoR reduce $\sigma^2_{\mathcal{LRS}}$. Indeed we show that for $\mathbf{L}$ an *age-parity* MPPM embedding *individual* costs and $\mathbf{L}^{\text{fold}}_{\text{age}}$ (denoted $\mathbf{L}^*$ in this section and the next, with a * as for the rest of the parameters related to the *folded* model) its *folded* daughter from which *individual* CoR are absent, we have

$$\sigma^2_{\mathcal{LRS}}(\mathbf{L}) \leq \sigma^2_{\mathcal{LRS}}(\mathbf{L}^*). \tag{10}$$

This result is achieved by focusing on the parity distributions, at demographic stable-state, of the successive age-classes in both models. In other words, the *individual* costs buffer individual stochasticity.

Here we illustrate this by analyzing an (*age-parity-strategy*) MPPM incorporating *individual* costs for multiple strategies that do not interact (i.e., $\mu = 0$; the different strategies can be seen as corresponding to different populations). We therefore performed our investigation on multiple (*age-parity*) MPPMs, each corresponding to a specific *strategy* and each incorporating *individual* CoR. To better understand the effects of the *individual* costs on $\sigma^2_{\mathcal{LRS}}$ we plot, in Figure 1, the difference in variance for a *constructed* (*age-parity*) matrix $\mathbf{L}$ with the *individual* costs and its *folded* Reference Leslie Matrix ($\mathbf{L}^* = \mathbf{L}_{\mathbf{age}}^{\mathbf{fold}}$) without the costs, for a range of zero-parity fertility and survival rates. More precisely, Figure 1a depicts the difference in variance $\sigma^2_{\mathcal{LRS}}(\mathbf{L}^*) - \sigma^2_{\mathcal{LRS}}(\mathbf{L})$ and Figure 1b the difference in coefficient of variation, $\frac{\sqrt{\sigma^2_{\mathcal{LRS}}}}{\mathbf{R_0}}(\mathbf{L}^*) - \frac{\sqrt{\sigma^2_{\mathcal{LRS}}}}{\mathbf{R_0}}(\mathbf{L})$. For reference, we also plot $\sigma^2_{\mathcal{LRS}}(\mathbf{L}^*)$ in Fig. 1c and the iso-fitness curves for both λ and $\mathcal{R_0}$ in Fig. 1d.
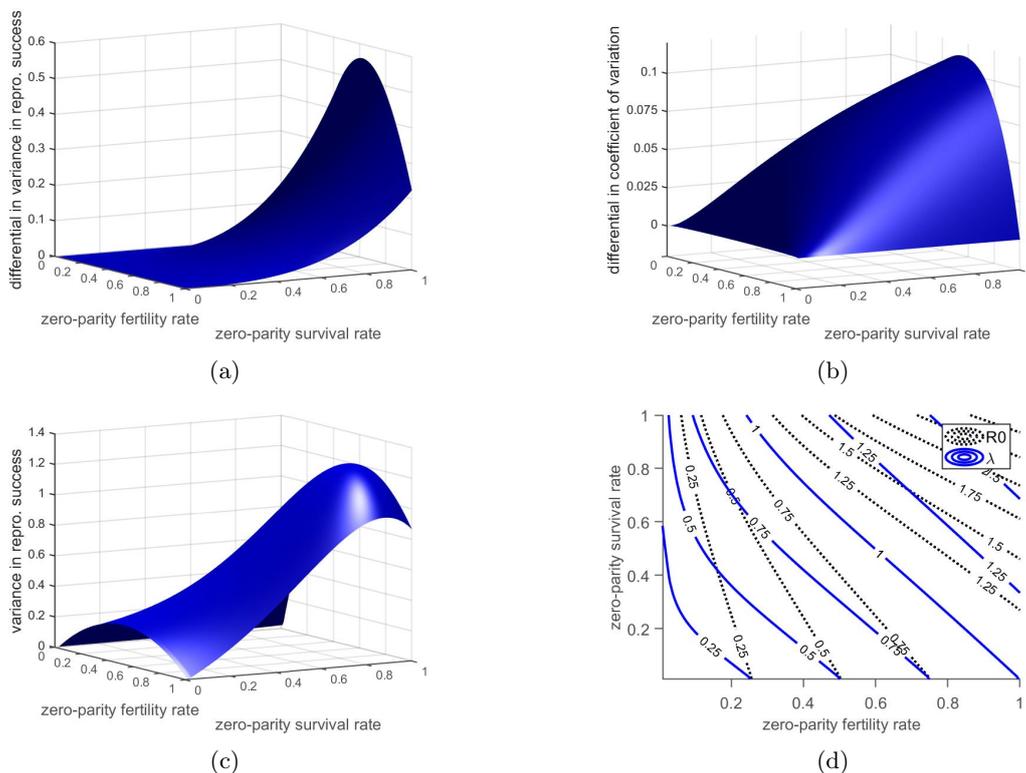

Figure 1: Effects of costs of reproduction on variance in lifetime reproductive success. For (*age-parity*) multitrait matrices implementing the *individual* costs (differing only in their zero-parity vital rates) and their related *folded* Reference Leslie Matrices from which they are absent, we plot the difference in variance (Fig.1a) and coefficient of variation (Fig.1b) of lifetime reproductive success between the two models. Fig.1c shows the variance in lifetime reproductive success for the Reference Leslie Matrix. Fig.1d shows the value of fitness measures $\mathcal{R_0}$ and λ for each combination of zero-parity vital rates. The population has maximum age $\omega = 5$ and age-at-maturity $\alpha = 1$. As per the generic model in this article, the *individual* costs is modeled by relatively decreasing each vital rate by $1/(1 + \omega - \alpha)$ per parity.

The first observation, is that individual CoR indeed reduce variance (Fig.1a) and coefficient of variation (Fig.1b) of $\mathcal{LRS}$. The second observation is that the effects of CoR on $\sigma^2_{\mathcal{LRS}}$ (fig.1a) follow the general shape of $\sigma^2_{\mathcal{LRS}}$ itself (fig.1c).

The shape of $\sigma^2_{\mathcal{LRS}}$ as a function of zero-parity rates f and s reveals that it results from the combined effects of three parameters. First, the variance in fertility rates at each age, $Var(\mathcal{F}^*_a) = f^*_a(1 - f^*_a)$, which is the "engine" of the variance in $\mathcal{LRS}$ and confers to the latter the $x(1-x)$ shape of the former along the zero-parity fertility rate axis. The importance of $Var(\mathcal{F}^*_a)$ for late ages however requires survival and thus the increase in $\sigma^2_{\mathcal{LRS}}$ as survival increases. At the same time, as age increases, we have, on average, a decrease in f^*_a because of the costs. Therefore even very high zero-parity fertility rates (conferring no variance in $\mathcal{F}_a$ at early ages) will generate variance at late ages. Hence, the asymmetrical $x(1-x)$ shape

8

at high survival rates, across fertility rates. Finally, survival does not only act as a promoter of variance in fertility, but as a stochastic process itself – of variance $s_i(1 - s_i)$ – which explains the decrease in variance as survival reaches its maximum levels. These last two effects, explain the general location, in this model, of the maximum $\sigma^2_{\mathcal{LRS}}$ (reached by organisms with zero-parity (survival, fertility) coordinates of $(s = 0.94, f = 0.64)$).

This general shape, namely the $x(1 - x)$ pattern on zero-parity fertility axis and general increase with survival, is preserved when switching from $\sigma^2_{\mathcal{LRS}}(\mathbf{L}^*)$ (Fig.1c) to $\sigma^2_{\mathcal{LRS}}(\mathbf{L}^*) - \sigma^2_{\mathcal{LRS}}(\mathbf{L})$ (Fig.1a). This is because this difference is a linear function of variance itself, as shown in Eq.(17) (Supplementary Material S.4). However this equation shows the difference in variance to also linearly depend on survival and fertility. This explains why the difference in variance between models with and without the costs (Fig.1a) increases with survival, even at high survival rates, and is flat at very low survival rates. These patterns are preserved when correcting for $\mathcal{R}_0$, i.e., for high fertility and survival rates, as can be observed from the differential in the coefficient of variation (Fig.1b). Logically both the exponential increase with survival and the asymmetrical effect for high fertility disappear.

These observations demonstrate that, even though very short-lived or semelparous organisms (i.e., with $s \approx 0$) exhibit variance in reproductive success (Fig. 1c), the *individual* CoR do not affect them (Fig. 1a and 1b) and that the effects of the costs will increase with iteroparity/longevity. Let us now investigate further the various effects of individual CoR on iso-fitness organisms across the slow–fast continuum.

3.2   Effects of *individual* CoR for iso-fitness organisms across the slow–fast continuum

From an evolutionary life history perspective, comparing the life histories of organisms with very different fitness makes little sense. Therefore, from the statistics plotted in Figure 1 for all possible zero-parity vital rates, we extract the combinations that are iso-fitness. More precisely, in Figure 2, we represent, for each possible zero-parity fertility rate, the corresponding zero-parity survival rate for a fitness of $\lambda \approx \mathbf{R}_0 \approx 1$ (red curve, right y-axis). For each such pair of coordinates, we extract the variances in $\mathcal{LRS}$ for the models with and without the costs (grey curves, left y-axis), and their difference (green curve, left y-axis).

This establishes, for the particular case of organisms that are iso-fitness, the general conclusions drawn above (here all organisms have stationary growth rate, and therefore $\mathcal{R}_0$ is worth unity): the variance in reproductive success stems from both variance in fertility and survival and is therefore maximal for intermediary values of f and s. However survival is also required to promote late fertility, and this pushes s_{max} higher and therefore f_{max} lower than the point of equal coordinates ($f = 0.54, s = 0.54$). As expected, because of the individual CoR, this is less true for $\mathbf{L}$, for which s_{max} is lower and therefore f_{max} higher, than for $\mathbf{L}^*$. To the contrary, the differential in variances between the two models (green curve) is maximal for the maximum possible survival rate $s = 1$ and its related zero-parity fertility-rate $f \approx 0.22$. In other words, this result shows that, whilst the effect of individual stochasticity is not a monotonous function of the pace of organisms as measured by their position on the slow–fast continuum (Stearns, 1983; Gaillard et al., 1989), the *effects* of *individual* CoR on such individual stochasticity increase with pace and are maximum for slow organisms.

3.3   Combining effects of *genetic* and *individual* costs on $\sigma^2_{\mathcal{LRS}}$

In Supplementary Material S.5, we demonstrate that *individual* costs and *fixed* heterogeneity (caused, e.g., by *genetic* costs) act independently and additively on $\sigma^2_{\mathcal{LRS}}$. In particular, the *fixed* heterogeneity component of the variance in lifetime reproductive success is unaffected by *individual* costs. In other words, this formally demonstrates the intuitive perception that *individual* costs act solely on the *dynamic* heterogeneity component of individual fitness variance. We also show there, that the *individual* costs increase the relative importance of the *fixed* (aka "adaptive") heterogeneity component of $\sigma^2_{\mathcal{LRS}}$ as it remains constant whilst the *dynamic* (aka "neutral") component of heterogeneity is reduced.

We illustrate this by providing $\sigma^2_{\mathcal{LRS}}$ and its decomposition for a numerical application of $\mathbf{L}$ (Expression 2). We call $\mathbf{L2}$, the MPPM for which age at first reproduction is $\alpha = 1$, maximum age $\omega = 15$, the zero-parity vital rates for the fast genotype $F = 0.35$ and $s = 0.6$ and for the slow genotype $f = 0.3$ and
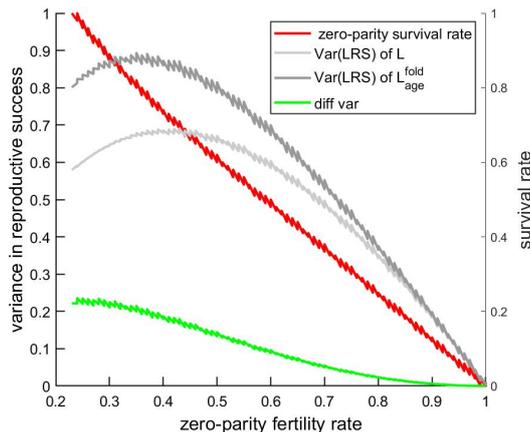
Figure 2: Effects of costs of reproduction on variance in lifetime reproductive success for stationary populations. For all combinations of zero-parity vital rates yielding an asymptotic growth rate $1 - \epsilon \leq \lambda \leq 1 + \epsilon$ (with $\epsilon = 0.01$), we plot, as a function of zero-parity fertility rates, the related zero-parity survival rate, the variance of reproductive output for the model implementing *individual* costs and that of its reference Leslie model with no trade-off implemented as well as their difference. The population has maximum age $\omega = 5$ and age-at-maturity $\alpha = 1$. Cost of reproduction is modeled by relatively decreasing each vital rate by $^1/(1 + \omega - \alpha)$ per parity.

$S = 0.8$. The decomposition of variance $\sigma^2_{\mathcal{LRS}}$ for **L2** and $\mathbf{L2^{fold}_{parity}}$, its folded version over parity from which *individual* costs are absent, yields:

$$\sigma^2_{\mathcal{LRS}}(\mathbf{L2^{fold}_{parity}}) = 1.2402 = \underbrace{1.2040}_{\sigma^{2dyn}_{\mathcal{LRS}}(\mathbf{L2^{fold}_{parity}})} + \underbrace{0.0362}_{\sigma^{2fix}_{\mathcal{LRS}}(\mathbf{L2^{fold}_{parity}})}$$

$$\sigma^2_{\mathcal{LRS}}(\mathbf{L2}) = 1.0802 = \underbrace{1.0439}_{\sigma^{2dyn}_{\mathcal{LRS}}(\mathbf{L2})} + \underbrace{0.0362}_{\sigma^{2fix}_{\mathcal{LRS}}(\mathbf{L2})}$$

We observe that, as expected, the *fixed* component of the variance decomposition i.e., the "adaptive" heterogeneity component, is small compared to the *dynamic*, i.e., "neutral", component. Here $\sigma^{2dyn}_{\mathcal{LRS}}$ represents 96.6% of $\sigma^2_{\mathcal{LRS}}$). As theoretically calculated also, the *fixed* component of the variance decomposition is preserved by *folding* over *parity*, i.e., when considering *individual* costs or not. Finally, and most importantly, we observe that the implementation of *individual* CoR increases the relative value of the "adaptive" component by 14.8% (the ratio of $0.0362/(1.204 + 0.0362)$ to $0.0362/(1.0439 + 0.0362)$).

Incorporating the *individual* components of the multiple LHTOs at play in an organism will increase this value further. This allows us to contemplate the "adaptive" component of individual heterogeneity as a stronger factor than sometimes anticipated (see Steiner and Tuljapurkar, 2012; Caswell, 2014; Cam et al., 2016; Snyder and Ellner, 2018; Hamel et al., 2018).

4   Discussion

In this article, we provide the steps allowing an ecologist to implement the *dynamic* and *fixed* components of a Life History Trade-Offs (LHTOs) into a MPPM, and to analyze their effects on the evolutionary dynamics of a population. Specifically, we focus on the two components – *individual* and *genetic* – of the Costs of Reproduction (CoR) and their effects on the variance in lifetime reproductive success, $\sigma^2_{\mathcal{LRS}}$. The random variable $\mathcal{LRS}$ is a commonly used measure of individual fitness and its expectation is the ubiquitous $\mathcal{R}_0 = E(\mathcal{LRS})$. The *genetic/fixed* component of CoR is caused by intra-population variance in pleiotropic genes acting on survival and fertility. In other words, it generates a gradient of strategies along the intra-population slow–fast continuum (Stearns, 1983; Gaillard et al., 1989). The *individual/dynamic* component of CoR is related to the variance in individual trajectories caused by individual stochasticity. Individuals of the same strategy may indeed exhibit different life trajectories. This is of course because of the randomness in vital rates, but also because the latter are affected, with stochasticity, by the *individual* costs, i.e., by the fact that past reproductive realizations negatively affect vital rates.

This general decomposition of LHTOs into *genetic/fixed* and *individual/dynamic* components is important for evolutionary demography as it is additive and can therefore be integrated into Population Projection Matrices (PPMs). Following this decomposition, we demonstrate how to generate a Multi-trait Population Projection Matrix (MPPM; Coste et al., 2017) incorporating these two components for the CoR. The *genetic* costs are embedded via a *fixed* trait that positions the lineage's *strategy*, slow or fast, along the slow–fast continuum. The *individual* costs are implemented via *dynamic* trait *parity*, the number of offspring ever born, that tracks individual reproductive success. By reducing the mean vital rates of individuals that have been successful so far in their life trajectory, *individual* costs control *dynamic* heterogeneity. The (*age-parity-strategy*) MPPM **L** is then analyzed via a Trait Level Analysis (TLA; Coste et al., 2017). It consists, in this case, in comparing the properties of the full model **L** with asymptotically equivalent *folded* versions of **L** from which traits *parity* and/or *strategy* are absent, and therefore where the related *dynamic* and/or *fixed* CoR are also concealed.

From this analysis, we formally demonstrate that *individual* CoR have a cushioning effect on the variance of reproductive success (Eq.10). We then investigate how the strategy of a lineage, its position on the *genetic* CoR, influences this buffering effect. We show that the *individual* costs have a stronger impact on the variance in reproductive success of long-lived organisms than on that of slow-lived organisms of the same fitness. For very short-lived ones, thus almost semelparous, the *individual* costs have almost no demographic buffering effect. Finally, as it reduces the variance in reproductive success, *individual* costs have a buffering effect on individual heterogeneity. We show, in this respect, that *individual* CoR only affect the *dynamic* component of $\sigma^2_{\mathcal{LRS}}$. Therefore, the dynamic component of the costs, which is often discarded to the benefit of its genetic/fixed counterpart, especially in comparative studies, acts solely on the "neutral" component of individual heterogeneity.

The key result in this paper, namely, the buffering effect of *individual* CoR on the *dynamic* component of the variance in reproductive success, has far reaching consequences for evolutionary demography, and, most importantly, for the measurement of the relative contributions of the *fixed* and *dynamic* component of individual heterogeneity via Integral Projection Models or PPMs. It implies that, when ecologists ignore the *individual* components of the multiple LHTOs at play in an organism, and only implements the *fixed* or *genetic* components, they compute a correct measure for the *fixed* component of heterogeneity, but overestimate the *dynamic* component (potentially to a large degree, if the organism is subject to many trade-offs). This forces evolutionary demographers to contemplate the "adaptive" (i.e., *fixed*) component of individual heterogeneity as a stronger factor than sometimes anticipated (see Steiner and Tuljapurkar, 2012; Caswell, 2014; Snyder and Ellner, 2018). Reintroducing Life History Trade-offs into the models of evolutionary demography might thus show that "luck" is not the only driver of individual heterogeneity and provide a potential way out to the debate in the evolutionary demography community about the relative importance of "adaptive" and "neutral" (i.e., *dynamic*) heterogeneities. Indeed, our theoretical model shows that it comes at no surprise that individual heterogeneity analyses accounting for different strategies (fixed component of trade-offs), but not incorporating individual components of trade-offs, yield a disproportionate importance for the "neutral" component of heterogeneity compared to the expectations of empiricists (Steiner and Tuljapurkar, 2012; Cam et al., 2016; Hamel et al., 2018).

From a methodological point of view, this study also highlights the strong limitation of life-history models which are only structured by *age*. It is often argued that these models are ideal to study populations for which age is the main determinant of life history. However this paradigm, we have shown here, has to be moved beyond. Firstly because trade-offs are a key component of life history and that, to be implemented, a trade-off requires at least two traits. Secondly, because age is only the best predictor of vital rates as it already encompasses some consequences of LHTOs. A model where vital rates do not depend on age, can seem to be strongly age-driven when *folded* upon the CoR. Using only one trait (partially incorporating, by linkage, the underlying trade-offs and thus seemingly a life history determinant) will generally provide appropriate results with respect to population dynamics and demography. It will however generate poor analyses from an evolutionary demography viewpoint. This can be readily ascertained by any empiricist when comparing the variance in reproductive success inferred by the Leslie Matrix generated from the Life History Table of her/his studied organism with actual statistics from the field. This discrepancy is only one in many consequences of interpreting *age*(only)-structured models without accounting for all the effects of the simplification.

It could therefore be argued that the addition of a 2nd trait in an age-structured model is as key to understand the life history of an organism from an evolutionary perspective, than the addition of the 1st trait (e.g. *age* or *stage*) – compared to a non-overlapping generation model – is from a demographic viewpoint. In general, this will prompt us to revisit general results stemming from one-trait analyses.

For instance, Charlesworth (1980) demonstrated that the *age*-structure of population has little impact on their population genetics. Would that result hold when a 2nd trait, implementing a constraint such as the *individual* costs, is added to the age-structured model ?

Appendices

A   Different models for the different components of trade-offs

The rarity of implementation of trade-offs into matrix projection models may be caused by the historical use of different families of models for population and individual mechanisms. Indeed mechanistic constraints, working at the individual level, are classically modeled via Individual-Based Models (IBMs; also called agent-based models) because they allow tracking each specific being during every step of its life trajectory (see for instance an IBM investigating CoR in ungulates by Proaktor et al. (2008)). Thanks to their level of details, such models can be considered as more precise and more flexible population projectors than matrices (Van Imhoff and Post, 1998). However, contrary to PPMs that project the population as a whole, they make it difficult to demonstrate the generalization of simulation results and to qualitatively ponder the weights of the various parameters that influence fitness (Caswell and John, 1992). By contrast, as their elementary elements are the vital rates for a given genotype (Engen et al., 2009; Csetenyi and Logofet, 1989; Williamson, 1959), PPMs are the ideal tool to implement *fixed/genetic* trade-offs: sensitivity analysis, measuring the effects of vital rates on demographic fitness, is at the core of evolutionary demography since Caswell (1978)'s matrix-based sensitivity formula.

Turning the argument around and considering that the state-specific vital rates observed for a population are the manifestations of an Evolutionary Stable Strategy (ESS; Parker and Maynard Smith, 1990), some authors use PPMs to infer the *fixed* trade-offs between various fitness components. This approach applies sensitivity analysis to ESS positions and was initiated by a series of articles about optimal life histories (Schaffer, 1974; Law, 1979; Caswell, 1982). It considers that the asymptotic growth rate (dominant eigenvalue λ_1 simplified as) λ – taken as fitness – is (locally) optimal, thus implying that vital rates changes are constrained by their sensitivity values. For example, a positive change in fertility at age α, $f(\alpha)$, would infer a negative change in survival at age β, $s(\beta)$, such that the ratio of changes (i.e., the magnitude of the trade-off) equals the ratio of sensitivities : $\frac{\partial \lambda}{\partial f(\alpha)} / \frac{\partial \lambda}{\partial s(\beta)}$; (see Caswell, 1982; Van Tienderen, 1995, for detailed analysis). This evolutionary demography approach, known as optimality theory, is very similar to the quantitative genetics method as demonstrated by Charlesworth (1990): if a population is at ESS then Lande (1982)'s equation becomes $0 = \mathbf{G}\nabla\boldsymbol{y}$, and therefore the genetic constraints between vital rates (in $\mathbf{G}$) stem directly from the selection gradient $\nabla\boldsymbol{y}$ corresponding to the vector of sensitivities of the asymptotic growth rate. However powerful optimality theory has proven to be in developing life history theory, such models *infer* but actually do not *incorporate* the *fixed* and *genetic* component of trade-offs.

B   Classical classification of LHTOs

The classical classification of trade-offs (see Stearns, 1992; Roff, 1993) is field-based. In that typology, they are segregated into "non-evolutionary" and "evolutionary" trade-offs. "Non-evolutionary" LHTOs are themselves split between "internal" or "physiological" trade-offs (when the trade-off stems from a constraint internal to the organism, for instance generated by Y-shaped allocation mechanism because of finite resources) and "external" or "ecological" LHTOs (when the constraint is caused by the environment). "Evolutionary" or "genetic" trade-offs correspond to a constraint located at the genotypic level (using Stearns (1989)'s genotypic/intermediate/phenotypic classical representation of LHTOs).

This classification is however not absolutely segregating, and not additive. It is indeed easy to find examples of "physiological" trade-offs that are *also* "genetic". Actually most of the early evolutionary demography studies of "physiological" trade-offs in the 70s (e.g. Schaffer, 1974) are really about "genetic" LHTOs as they do not study the "physiological"/individual aspects of the constraint, but how genes acting on the allocation of resources towards various fitness functions will evolve under various circumstances. Indeed, in these articles, two individuals with the same genotype, or clones, are deemed to exhibit the same life trajectories. The trade-off are called "physiological" there, because that is *where* the constraint is supposedly located, but "genetic" and "ecological" trade-offs (e.g., an antagonistic pleiotropy in genes generating a trade-off between functions without any physiological inter-mediation, potentially with a

behavioral mediation) would yield the same results. The "location" of the constraint, as explained in the Introduction, is much less important for theoretical analyses of trade-offs than the origin of the variance in the traits involved in the trade-offs. Under the arising new additive and segregating typology (see second paragraph of the Introduction), therefore, such trade-offs would be classified as *genetic*.

C   Implementation of LHTOs into MPPMs with empirical data

The decomposition of LHTOs into *genetic* and *individual* components hints at empirical determinations of their parameters as can be inferred from their relationship with the decomposition of individual heterogeneity into, respectively, *fixed* and *dynamic* components. The methods developed to weight each component of heterogeneity from empirical data (see review in Hamel et al., 2018) can indeed be extended to evaluate the strength of each component of LHTOs at play. The implementation can be sequenced as follows:

- The first step consists in splitting the population into subgroups with (significantly) different *strategies* (i.e. positions on the *genetic component* of LHTO). For instance, for the quality/quantity trade-off, this process would yield subgroups with consistently more numerous and more fragile offspring than others. Embedding such a *genetic component* is done the same way as implementing different *fixed* heterogeneities. In order to be able to analyze the population over long periods of time ($>$ generation time) or asymptotically, knowledge of heredity of *fixed* traits is required (Plard et al., 2018). However if only individual trajectories are of interest, then heredity may be dispensed (Jenouvrier et al., 2017). The decomposition into such *fixed*-heterogeneity subgroups is classically done by mixture models (Hamel et al., 2018)

- The second step consists, for each of the *strategies* (i.e., *fixed*-heterogeneity groups) identified in the first step, to measure the modalities and the strength of the *individual component* of the trade-off. For instance, for the quantity/quality trade-off, this would consist, for each "lineage" on the intraspecific quantity-quality spectrum, in gathering statistics on the effects of the number of early-life offspring and their survival onto later-life quantity and quality of juveniles. This analysis of *dynamic* heterogeneity can be extracted from joint models (Hamel et al., 2018). An interesting illustration, in the literature, of analysis of the *individual* component of a LHTO was performed by Miller et al. (2012) who quantify the effects of flowering or producing a fruit in year $t - \tau$ onto growth, survival and dormancy in year t of orchid *Orchis purpurea* via generalized linear mixed effects models.

When the traits under consideration are continuous, ecologists will resort to multitrait Integral Projection Models, themselves yielding MPPMs, as described by Ellner and Rees (2006) and Vindenes and Langangen (2015).

Acknowledgments

Bibliography

References

Cam, E., Aubry, L. M., and Authier, M. (2016). The conundrum of heterogeneities in life history studies. *Trends in Ecology & Evolution*, 31(11):872–886.

Caswell, H. (1978). A general formula for the sensitivity of population growth rate to changes in life history parameters. *Theoretical Population Biology*, 14(2):215–230.

Caswell, H. (1982). Optimal life histories and the age-specific costs of reproduction. *Journal of theoretical biology*.

Caswell, H. (2009). Stage, age and individual stochasticity in demography. *Oikos*, 118(12):1763–1782.

Caswell, H. (2011). Beyond R0: Demographic models for variability of lifetime reproductive output. *PLoS ONE*, 6(6):e20809.

Caswell, H. (2014). A matrix approach to the statistics of longevity in heterogeneous frailty models. *Demographic Research*, 31(1):553–592.

Caswell, H. and John, A. M. (1992). From the individual to the population in demographic models. *Individual-based models and approaches in ecology. Springer US, 1992. 36-61*, pages 36–61.

Caswell, H., Neubert, M. G., and Hunter, C. M. (2011). Demography and dispersal: invasion speeds and sensitivity analysis in periodic and stochastic environments. *Theoretical Ecology*, 4(4):407–421.

Charlesworth, B. (1980). *Evolution in age structured populations*. Cambridge University Press.

Charlesworth, B. (1990). Optimization models, quantitative genetics, and mutation. *Evolution*, 44(3):520–538.

Cody, M. L. (1966). A general theory of clutch size. *Evolution, 20, 174-194.*, 20(2):174–184.

Coste, C. F. D., Austerlitz, F., and Pavard, S. (2017). Trait level analysis of multitrait population projection matrices. *Theoretical Population Biology*, 116:47–58.

Csetenyi and Logofet, D. O. (1989). Leslie model revisited: some generalizations to block structures. *Ecological Modelling*, 48:277–290.

de Kroon, H., Plaisier, A., van Groenendael, J., and Caswell, H. (1986). Elasticity: the relative contribution of demographic parameters to population growth rate. *Ecology*, 67(5):1427–1431.

de Vries, C. and Caswell, H. (2019). Stage-structured evolutionary demography: linking life histories, population genetics, and ecological dynamics. *The American Naturalist*, 193(4):000–000.

Ellner, S. P. and Rees, M. (2006). Integral projection models for species with complex demography. *The American Naturalist*, 167(3):410–428.

Engen, S., Lande, R., and Saether, B.-E. (2009). Reproductive value and fluctuating selection in an age-structured population. *Genetics*, 183(2):629–37.

Enright, N. J., Franco, M., and Silvertown, J. (1995). Comparing plant life histories using elasticity analysis : theimportance of life span and the number of life - cycle stages. *Oecologia*, 104(1):79–84.

Gaillard, J.-M., Pontier, D., Allainé, D., Lebreton, J.-D., Trouvilliez, J., and Clobert, J. (1989). An analysis of demographic tactics in birds and mammals. *Oikos*, 56(1):59–76.

Giske, J., Aksnes, D. L., and Førland, B. (1993). Variable generation times and Darwinian fitness measures. *Evolutionary Ecology*, 7(3):233–239.

Goodman, L. A. (1971). On the sensitivity of the intrinsic growth rate to changes in the age-specific birth and death rates. *Theoretical Population Biology*, 2(3):339–354.

Hamel, S., Gaillard, J.-m., Yoccoz, N. G., Bassar, R. D., Bouwhuis, S., Caswell, H., Douhard, M., Gangloff, E. J., Gimenez, O., Lee, P. C., Smallegange, I. M., Steiner, U. K., Vedder, O., and Vindenes, Y. (2018). General conclusion to the special issue Moving forward on individual heterogeneity. *Oikos*, 127(5):750–756.

Hatori, H. (1966). On Markov chains with rewards. *Kodai Mathematical Seminar Reports*, 18(2):184–192.

Hooley, D. E. (2000). Collapsed Matrices with (Almost) the Same Eigenstuff. *The College Mathematics Journal*, 31(4):297.

Howard, R. A. (1960). *Dynamic Programming and Markov Processes*, volume 3. The M.I.T. Press, Cambridge, Massachusetts.

Jenouvrier, S., Aubry, L. M., Barbraud, C., Weimerskirch, H., and Caswell, H. (2017). Interacting effects of unobserved heterogeneity and individual stochasticity in the life-history of the Southern fulmar. *Journal of Animal Ecology*, 38(1):42–49.

Jessup, C. M. and Bohannan, B. J. (2008). The shape of an ecological trade-off varies with environment. *Ecology Letters*, 11(9):947–959.

Lack, D. (1954). The evolution of reproductive rates. In Huxley, J., Hardy, A., and Ford, E., editors, *Evolution as a Process*, pages 143–156. Allen and Unwin, London.

Lande, R. (1982). A quantitative genetic theory of life history evolution. *Ecology*, 63(3):607–615.

Law, R. (1979). Optimal life histories under age-specific predation. *The American Naturalist*, 114(3):399–417.

McGraw, J. B. and Caswell, H. (1997). Estimation of individual fitness from life history data.

Metz, J. A. J. and Diekmann, O. (1986). *The dynamics of physiologically structured populations*. Springer.

Miller, T. E. X., Williams, J. L., Jongejans, E., Brys, R., and Jacquemyn, H. (2012). Evolutionary demography of iteroparous plants: incorporating non-lethal costs of reproduction into integral projection models. *Proceedings of the Royal Society B: Biological Sciences*, 279(1739):2831–2840.

Murray, B. G. (1992). The evolutionary significance of lifetime reproductive success. *The Auk*, 109(1):167–172.

Nur, N. (1984). The consequences of bood size for breeding blue tits II. Nestling weight, offspring survival and optimal brood size. *The Journal of Animal Ecology*, 53(2):497.

Orton, J. H. (1929). Reproduction and death in invertebrates and fishes. *Nature*, 3088(123):14–15.

Parker, G. and Maynard Smith, J. (1990). Optimality theory in evolutionary biology. *Nature*, 348:27–33.

Plard, F., Schindler, S., Arlettaz, R., and Schaub, M. (2018). Sex-specific heterogeneity in fixed morphological traits influences individual fitness in a monogamous bird population. *The American Naturalist*, 191(1):106–119.

Proaktor, G., Coulson, T., and Milner-Gulland, E. J. (2008). The demographic consequences of the cost of reproduction in ungulates. *Ecology*, 89(9):2604–2611.

Rees, M., Childs, D. Z., and Ellner, S. P. (2014). Building integral projection models: A user's guide. *Journal of Animal Ecology*, 83(3):528–545.

Roff, D. A. (1993). *Evolution Of Life Histories: Theory and Analysis*. Springer USA.

Roff, D. A. and Fairbairn, D. J. (2007). The evolution of trade-offs: Where are we? *Journal of Evolutionary Biology*, 20(2):433–447.

Roth, G. and Caswell, H. (2016). Hyperstate matrix models: extending demographic state spaces to higher dimensions. *Methods in Ecology and Evolution*, 7(12):1438–1450.

Salguero-Gómez, R. and Plotkin, J. B. (2010). Matrix dimensions bias demographic inferences: implications for comparative plant demography. *The American naturalist*, 176(6):710–722.

Schaffer, W. M. (1974). Selection for optimal life histories: the effects of age structure. *Ecology*, 55(2):291–303.

Snyder, R. E. and Ellner, S. P. (2018). Pluck or luck: Does trait variation or chance drive variation in lifetime reproductive success? *The American Naturalist*, 191(4):E000–E000.

Stearns, S. C. (1983). The influence of size and phylogeny on patterns of covariation among life-history traits in the mammals. *Oikos*, 41(2):173–187.

Stearns, S. C. (1989). Trade-offs in life-history evolution. *Functional Ecology*, 3(1974):259–268.

Stearns, S. C. (1992). *The evolution of life histories*, volume 1. Oxford University Press.

Steiner, U. K. and Tuljapurkar, S. (2012). Neutral theory for life histories and individual variability in fitness components. *Proceedings of the National Academy of Sciences*, 109(12):4684–4689.

Steiner, U. K., Tuljapurkar, S., and Orzack, S. H. (2010). Dynamic heterogeneity and life history variability in the kittiwake. *Journal of Animal Ecology*, 79(2):436–444.

Tuljapurkar, S. and Steiner, U. K. (2010). Dynamic heterogeneity and life histories. *Annals of the New York Academy of Sciences*, 1204(1):65–72.

Tuljapurkar, S., Steiner, U. K., and Orzack, S. H. (2009). Dynamic heterogeneity in life histories. *Ecology Letters*, 12(1):93–106.

Van Imhoff, E. and Post, W. (1998). Microsimulation methods for population projection. *Population: An English Selection*, 10(1):97–138.

Van Tienderen, P. H. (1995). Life cycle trade-offs in matrix population models. *Ecology*, 76(8):2482–2489.

Vindenes, Y. and Langangen, Ø. (2015). Individual heterogeneity in life histories and eco-evolutionary dynamics. *Ecology Letters*, 18(5):417–432.

Williamson, M. H. (1959). Some extensions of the use of matrices in population theory. *The Bulletin of Mathematical Biophysics*, 21(1):13–17.

Supplementary Materials

S.1 Note on matrix $\mathbf{L^{fold}_{age,parity}}$: vital rates, $\mathcal{R}_0$ and interpretation

Matrix $\mathbf{L^{fold}_{age,parity}}$ is matrix $\mathbf{L}$, the *age-parity-strategy* MPPM, *folded* over *strategy*. In $\mathbf{L^{fold}_{age,parity}}$, *fixed* heterogeneity is not implemented as a trait any more, but since it was implemented in the full-traited matrix $\mathbf{L}$ from which it is derived, it has effects on $\mathbf{L^{fold}_{age,parity}}$, making its interpretation both challenging and interesting.

Discrepancies in calculation of $\mathcal{R}_0$

In $\mathbf{L}$, because of the implementation of *individual* costs via trait *parity*, survival transitions output states depend on fertility. Simply put, survival transitions from any state $i = (a, p, st)$ to either $j_1 = (a+1, p, s)$ or $j_2 = (a+1, p+1, s)$ are $\mathrm{L}_{j_1,i} = s_i \times (1 - f_i)$ and $\mathrm{L}_{j_2,i} = s_i \times f_i$, with a third, implicit, transition towards *death* equal to $\tilde{\mathrm{M}}_{death,i} = 1 - s_i$. These three transitions sum to 1. In the MCwR tool, the corresponding fertility rewards expectations for these three transitions (in $\mathbf{Rw^1}$) are respectively 0, 1 and f_i. Thus the mean expected reward is $0 \times (s_i(1 - f_i)) + 1 \times (s_i f_i) + f_i(1 - s_i) = f_i$ and therefore both MCwR and $\mathbf{R}$ approaches provide the same results for $E(\mathcal{LRS})$. In $\mathbf{L^{fold}_{age}}$, the Leslie reference matrix, survival and fertility transitions are completely separated, with only one output per survival transition. Thus, in this case also, both MCwR and $\mathbf{R}$ provide the same results. However for the intermediary matrix, $\mathbf{L^{fold}_{age,parity}}$, which is $\mathbf{L}$ *folded* on *strategy*, both measures differ. Indeed, through *folding*, the survival transitions from state $i = (a, p)$ towards either $j_1 = (a+1, p)$ or $j_2 = (a+1, p+1)$ will, in general, not be distributed according to the transition value between i and the (unique) offspring state 1 which we interpret as fertility rate ($\mathrm{L}_{1,i \leftrightarrow (a,p)} = f_i$). This is caused by the *fixed* heterogeneity modeled in $\mathbf{L}$ expressing itself through EFP-*merged* vital rates, now that *strategy* is not a trait any more (see Coste et al., 2017).

Let us illustrate this, seemingly paradoxical, situation with a simple example: imagine a population structured by 2 *age* (and therefore 2 *parity*) and 2 *heterogeneity* classes (A and B) produced in equal measures ($\mu = 0.5$) at each fertility event. A individuals have all vital rates at 1 and B individuals at 0.5. Then all A newborns (half the population of newborns), will produce 1 offspring and become individuals of age 2 and parity 1. Half of B newborns will produce 1 offspring and half of B individuals will survive. Those halves are independent, and thus a quarter of B individuals will survive *and* become adults of *parity* 1, and another quarter will become adults of *parity* 0. Thus for the population *folded* on *strategy*, i.e., where individuals are only characterized by *age* and *parity*, the newborn fertility rate is $0.5 \times 1 + 0.5 \times 0.5 = 0.75$. Similarly the survival rate for newborns is $0.5 \times 1 + 0.5 \times 0.5 = 0.75$. However, for an average newborn in the population, the probability of transitioning towards a *parity* 1 adult is $0.5 \times 1 + 0.5 \times 0.25 = 0.625$ and to a *parity* 0 adult is $0.5 \times 0 + 0.5 \times 0.25 = 0.125$. As we can see here, the sum of the survival transitions is (by construction) equal to the survival rate, but the distribution towards higher parity $\frac{0.625}{0.625+0.125} \approx 0.83$ is not equal to the fertility rate 0.85 as one does not make the distinction between individuals A and B any more.

Interpretation of $\mathbf{L^{fold}_{age,parity}}$

These considerations have important consequences with regards to the interpretation of $\mathbf{L^{fold}_{age,parity}}$. It basically comes down to deciding whether fertility rates are to be found on the first line of the matrix, or in the distribution rates towards classes of higher *parity*. In the first case, $E(\mathcal{LRS})$ should be calculated using $\mathcal{R}_0 = \mathrm{R}_{1,1}$, where $\mathbf{R}$ is the next generation matrix; in the second case, via MCwR. Because, as we just illustrated, the "inferred" fertility rates are, in general, different between fertility transition and distribution of survival transition, these two methods provide different results for $\mathcal{R}_0$. Considering that the *folding* operation does not alter the fact that $\mathbf{L^{fold}_{age,parity}}$ is an *age*-based MPPM with no *fixed* heterogeneity implemented, and thus only 1 offspring class, it makes sense to resolve the dispute in favor of considering the first line of the matrix as fertility rates for all states. Then, however, it implies that, the second trait of the model is abusively called *parity*. The categories it generates still correspond to states with decreasing vital rates as the category number increases (i.e., to *individual* CoR on survival and fertility), but an increment in the category number does not imply 1 exact additional offspring. The relationship is not linear any more, and the trait *parity* rather becomes a general "measure of overall reproductive success" than parity exactly, though we will still use that name for the trait itself.

That the second trait of $\mathbf{L^{fold}_{age,parity}}$ cannot be interpreted as parity *stricto sensu* also has repercussions in terms of measures for the variance of $\mathcal{LRS}$. We just saw that MCwR cannot be used to measure $E(\mathcal{LRS})$, and, for the same reason, this framework cannot be used for precisely calculating $\sigma^2_{\mathcal{LRS}}$ either.

Moreover, even if *parity* does not account exactly for the reproductive success any more, there is still interdependence between fertility rates and survival transitions, making the formulas stemming from $\mathbf{R}$ equally unsatisfactory. We can therefore use both approaches, as proxies, keeping in mind that none can provide an exact result, which reflects the fact that matrix $\mathbf{L}^{\text{fold}}_{\text{age,parity}}$ is not a constructed model, but the product of *folding* from a model embedding an *individual* trade-off, implying a shift in the interpretation of its *dynamic* trait.

S.2 General non-preservation of $\mathcal{R}_0$ by *folding*

Consider two categories/traits, t_1 and t_2, each having 2 classes, and where there is only 1 offspring state: $(1,1)$. Let us further consider that the $(t_1\text{-}t_2)$ MPPM for this population is: $\mathbf{L3} = \begin{bmatrix} 0.6 & 0.6 & 0.6 & 0.6 \\ 0.5 & 0 & 0 & 0 \\ 0 & 0 & 0.5 & 0 \\ 0 & 0.5 & 0 & 0 \end{bmatrix}$. Then we get $\lambda_{\mathbf{L3}} = 1.0317$ and – by letting $\mathbf{F3}$ be the empty matrix but with the first line of $\mathbf{L3}$, $\mathbf{T3}$ the complement of $\mathbf{F}$ in $\mathbf{L3}$, $\mathbf{N3} = (\mathbf{I} - \mathbf{T3})^{-1}$ the fundamental matrix and $\mathcal{R}_0[\mathbf{L3}]$ the first element of $\mathbf{R3} = \mathbf{F3}.\mathbf{N3}$ – we get $\mathcal{R}_0[\mathbf{L3}] = 1.05$. The eigen-analysis of $\mathbf{L3}$ allows us to fold it over t_1 , and we get $\mathbf{L3}^{\text{fold}}_{\mathbf{t_2}} = \begin{bmatrix} 0.9368 & 0.6 \\ 0.1632 & 0 \end{bmatrix}$.

The computation of the eigenvalues of $\mathbf{L3}^{\text{fold}}_{\mathbf{t_2}}$ yields, as expected, $\lambda_{\mathbf{L3}^{\text{fold}}_{\mathbf{t_2}}} = 1.0317 = \lambda_{\mathbf{L3}}$. By construction, in this matrix also, offspring are only to be found on the first line. And therefore, we can proceed as we just did for $\mathbf{L3}$, to generate the net reproductive rate, and we get $\mathcal{R}_0[\mathbf{L3}^{\text{fold}}_{\mathbf{t_2}}] = 1.035$. This simple model illustrates the general non-preservation of $\mathcal{R}_0$ by EFP *folding*.

S.3 $\mathcal{R}_0$ preserved by *folding* for *age*-structured populations

We demonstrate here that for MPPMs with *age* as a trait, $\mathcal{R}_0$ is preserved by *folding* (over any combination of traits other than *age*). This may seem self-evident, but it really is not (see Appendix S.2).

To prove the preservation of $\mathcal{R}_0$ by *folding* in the specific case where *age* is a trait and is not *folded* upon, let us consider a model $\mathbf{L}$, that is re-organized (if need be) so that *age* is the last trait in the "trait structure" $\mathbf{s}$ (see Coste et al., 2017). Let us regroup all other traits as one unique trait t which can take values from $t = 1$ to $t = tmax$, representing the $tmax$ combinations of other (than *age*) traits. Trait vector is thus $\mathbf{t} = \{t, age\}$ and trait structure $\mathbf{s} = (tmax, \omega)$ (there are ω age classes). With no loss of generality therefore, we shall study the effect, on $\mathcal{R}_0$, of *folding* $\mathbf{L}$ over t . The operation produces $\mathbf{L}^{\text{fold}}_{\text{age}} = \mathbf{L_a}$ only characterized by age: $\mathbf{t_{L_a}} = \{age\}$ and trait structure $\mathbf{s_{L_a}} = (\omega)$. For simplicity, we shall use a block-matrix approach for the demonstration. Matrix $\mathbf{L_a}$ is a Leslie matrix: $\mathbf{L_a} = \begin{bmatrix} f_1 & f_2 & \cdots & f_\omega \\ s_1 & 0 & \cdots & 0 \\ \cdots & \cdots & \cdots & \cdots \\ 0 & 0 & s_{\omega-1} & 0 \end{bmatrix}$ with well-know net reproductive rate, we denote $\mathbf{R_0^*}$: $\mathbf{R_0^*} = \sum_{i=1}^{\omega} f_i (\prod_{j=1}^{i-1} s_j)$.

Matrix $\mathbf{L}$ can be written a block-Leslie matrix :

$$\mathbf{L} = \left[\begin{array}{c|c|c|c|c} \mathbf{F}_1 & \mathbf{F}_2 & \dots & \mathbf{F}_{\omega-1} & \mathbf{F}_\omega \\ \hline \mathbf{S}_1 & \mathbf{0} & \dots & \mathbf{0} & \mathbf{0} \\ \hline \dots & \dots & \dots & \dots & \dots \\ \hline \mathbf{0} & \mathbf{0} & \mathbf{0} & \mathbf{0} & \mathbf{0} \\ \hline \mathbf{0} & \mathbf{0} & \dots & \mathbf{S}_{\omega-1} & \mathbf{0} \end{array} \right] \quad ,$$

where each submatrix is a square matrix of size $tmax \times tmax$. Specifically, each is such that for a vector $\boldsymbol{n_i}$ of abundances of individuals of age i, $\mathbf{F}_i.\boldsymbol{n_i}$ is the vector of abundances of offspring produced by these individuals at a given time step and $\mathbf{S}_i.\boldsymbol{n_i}$ is the vector of abundances of their survived selves. By construction $\mathbf{L}$ and $\mathbf{L_a}$ share the same growth rate λ. Their related right eigenvectors, both summing to 1, $\boldsymbol{w} = \begin{bmatrix} \boldsymbol{w_1} & \boldsymbol{w_2} & \dots & \boldsymbol{w_\omega} \end{bmatrix}$ (this formula displays $\boldsymbol{w}$ as a vector of vectors) and $\boldsymbol{w^*} = \begin{bmatrix} w_1^* & w_2^* & \dots & w_\omega^* \end{bmatrix}$ are such that $\mathbf{1'}.\boldsymbol{w_i} = w_i^*$. We get (we allow ourselves to equate matrices of different sizes whenever they have equal non-zero diagonal block-matrices on their Frobenius normal form):

$$\mathbf{R_0} = \frac{\mathbf{1'R}\boldsymbol{w_1}}{w_1^*}. \tag{11}$$

Writing out $\mathbf{R}$, we get :

$$\mathbf{R} = \mathbf{F}(\mathbf{I} + \mathbf{T} + \mathbf{T^2} + \cdots + \mathbf{T^\omega}) = \sum_{i=1}^{\omega} \mathbf{F}_i \mathbf{P}_i. \tag{12}$$

where $\mathbf{P}_i = \prod_{j=i-1}^{j=1} \mathbf{S}_i$ (order of multiplicands is important here) and $\mathbf{P}_1 = \mathbf{I}$. Then from Eqs. (12) and (11) we get :

$$\mathbf{R_0} = \mathbf{1}' \sum_{i=1}^{\omega} \mathbf{F}_i \mathbf{P}_i \frac{\boldsymbol{w_1}}{w_1^*} = \sum_{i=1}^{\omega} \mathbf{1}' \mathbf{F}_i \mathbf{P}_i \frac{\boldsymbol{w_1}}{w_1^*}. \tag{13}$$

Considering the eigen-equation $\mathbf{L}\boldsymbol{w} = \lambda \boldsymbol{w}$ by blocks, we immediately get $\mathbf{S_i}\boldsymbol{w_i} = \lambda \boldsymbol{w_{i+1}}$ and $\sum_{i=1}^{\omega} \mathbf{F}_i \boldsymbol{w_i} = \lambda \boldsymbol{w_1}$. The eigen-equation at the level of $\mathbf{L_{age}^{fold}}$, $\mathbf{L_a} \boldsymbol{w^*} = \lambda \boldsymbol{w^*}$, implies that $s_i w_i^* = \lambda w_{i+1}^*$. Thus $\mathbf{S_i} \frac{\boldsymbol{w_i}}{w_i^*} = s_i \frac{\boldsymbol{w_{i+1}}}{w_{i+1}^*}$. Therefore, we infer

$$\mathbf{P}_i . \frac{\boldsymbol{w_1}}{w_1^*} = \left(\prod_{j=1}^{i-1} s_j\right) \frac{\boldsymbol{w_i}}{w_i^*}. \tag{14}$$

By extension of EFP *folding* (see Coste et al., 2017) we know that the *folding* of matrices consist of the asymptotic-abundance-weighted averaging of transitions. For fertility, the transitions are to be found in the matrices $\mathbf{P}_i$ and the corresponding asymptotic abundances in the vectors $\boldsymbol{w_i}$, therefore:

$$f_i = \mathbf{1}' \mathbf{F}_i . \frac{\boldsymbol{w_i}}{w_i^*}. \tag{15}$$

Multiplying both sides of Eq. (14) by $\mathbf{1}' \mathbf{F}_i$, and simplifying the result thanks to Eq. (15), we can rewrite Eq. (13) in a way that provides the proof:

$$\mathbf{R_0} = \sum_{i=1}^{\omega} f_i \left(\prod_{j=1}^{i-1} s_j\right) = \mathbf{R_0^*}. \tag{16}$$

S.4   Demonstration of $\sigma^2_{\mathcal{LRS}} \left(\mathbf{L_{age,parity}} \right) < \sigma^2_{\mathcal{LRS}} \left(\mathbf{L_{age}^{fold}} \right)$

Let us consider an (*age-parity*)-model $\mathbf{L}$ implementing *individual* costs. Without loss of generality, for simplification, we shall consider that only fertility rates are affected by the costs. Let us also consider, $\mathbf{L_{age}^{fold}}$, which is $\mathbf{L}$ folded on *parity*, that we denote here $\mathbf{L}^*$. In order to demonstrate that $\sigma^2_{\mathcal{LRS}} (\mathbf{L}) < \sigma^2_{\mathcal{LRS}} (\mathbf{L}^*)$, we shall set our investigation at the sable-state. By the properties of TLA, at the stable state, $\mathbf{L}$ and $\mathbf{L}^*$ have the same growth rate and the associated right-eigen vector on *age* $\boldsymbol{w_a}$. Let us denote $\mathcal{P}_a$ and $\mathcal{P}^*_a$ the random variables giving the parity of a random individual in the a age-class, in the stable state population, for respectively $\mathbf{L}$ and $\mathbf{L}^*$. The parity r.v. at age $(a+1)$ are worth $\mathcal{P}_{a+1} = \mathcal{S}_a \mathcal{F}_{a,p} + \mathcal{P}_a$ and $\mathcal{P}^*_{a+1} = \mathcal{S}^*_a \mathcal{F}^*_a + \mathcal{P}^*_a$.

We can get expectations for the r.v. of the multitrait model, according to parity. $E_p(\mathcal{P}_a) = \sum_{p=1}^{a} \frac{p.w_{a,p}}{w_a}$ is $\bar{p}_a$ the average parity at that age a. $E_p(\mathcal{F}_{a,p}) = \sum_{p=1}^{a} \frac{f(a,p)w_{a,p}}{w_a}$. Since $f(a,p) = f_a(1-\frac{p}{\omega})$, and from the TLA principles, we have $E_p(\mathcal{F}_{a,p}) = \frac{f_a}{w_a} \sum_{p=1}^{a}(1-\frac{p}{\omega})w_{a,p} = \frac{f_a}{w_a} \left(\sum_{p=1}^{a} w_{a,p} - \frac{1}{\omega}\sum_{p=1}^{a} p \right) = f_a(1-\frac{\bar{p}_a}{\omega}) = E(\mathcal{F}^*_a) = \bar{f}_a = f_a^*$. From the summation of $E(\mathcal{P}_{a+1}) = E(\mathcal{S}_a).E(\mathcal{F}_{a,p}) + E(\mathcal{P}_a)$ over a, we therefore get $\forall a \ E_p(\mathcal{P}_a) = E(\mathcal{P}^*_a)$. This result is related to the preservation of $\mathbf{R_0}$ we demonstrate in section S.3. To simplify further calculations, as we base our analysis at the timestep level, we shall now consider only one process projecting an individual from age a to $a+1$, which combines fertility and survival: $\mathcal{Q}_{a,p} = \mathcal{S}_a \mathcal{F}_{a,p}$. As a product of Bernoulli processes, $\mathcal{Q}$ is itself Bernoulli, of parameter $q_{a,p} = f_a s_a(1-\frac{p}{\omega})$.

Let us now turn ourselves to the variances of these r.v., since in a population structured by age only, the vital rates are independent from parity, we have $Var_p(\mathcal{P}^*_{a+1}) = Var_p(\mathcal{Q}^*_a) + Var_p(\mathcal{P}^*_a)$ and thus $Var_p(\mathcal{P}^*_{a+1}) - Var_p(\mathcal{P}^*_a) = q_a^*(1-q_a^*)$. We also have : $Var_p(\mathcal{P}_{a+1}) = Var_p(\mathcal{Q}_a) + Var_p(\mathcal{P}_a) + 2Cov_p(\mathcal{Q}_a, \mathcal{P}_a)$. As $\mathcal{Q}$ is Bernoulli, we have $Var_p(\mathcal{Q}_a) = \sum_{p=1}^{a} 1^2 q(p).w_{a,p} - (q_a^*)^2 = q_a(1-q_a) = Var_p(\mathcal{Q}^*_a)$. And therefore, the difference in change in variances, by age, lies in the covariance $Cov(\mathcal{F}_a, \mathcal{P}_a)$ component:

$$(Var_p(\mathcal{P}_{a+1}) - Var_p(\mathcal{P}_a)) - \left(Var_p(\mathcal{P}^*_{a+1}) - Var_p(\mathcal{P}^*_a)\right) = 2Cov_p(\mathcal{Q}_a, \mathcal{P}_a)$$

We can explicit this component :

$$Cov(\mathcal{Q}_a, \mathcal{P}_a) = \sum_{p=1}^{a} p.q(a,p)w_{a,p} - \bar{p}_a q_a^*$$

where

$$\sum_{p=1}^{a} pq(a,p)w_{a,p} = q(a)\sum_{p=1}^{a} p(1-\frac{p}{\omega})w_{a,p} = q(a)\sum_{p=1}^{a} pw_{a,p} - \frac{1}{\omega}q(a)\sum_{p=1}^{a} p^2 w_{a,p}$$

$$= q(a)\bar{p_a} - \frac{1}{\omega}q(a)\sum_{p=1}^{a} p^2 w_{a,p} = [q(\bar{a}) + q(a)\frac{p_a}{\omega}].\bar{p_a} - \frac{1}{\omega}q(a)\sum_{p=1}^{a} p^2 w_{a,p}$$

and thus

$$Cov_p(\mathcal{Q}_a, \mathcal{P}_a) = \frac{q_a}{\omega}\left(\bar{p_a}^2 - \sum_{p=1}^{a} p^2 w_{a,p}\right) = \frac{q_a}{\omega}(-Var_p(\mathcal{P}_a))$$

And therefore,

$$(Var_p(\mathcal{P}_{a+1}) - Var_p(\mathcal{P}_a) - \left(Var_p(\mathcal{P}_{a+1}^*) - Var_p(\mathcal{P}_a^*\right) = 2\frac{f_a s_a}{\omega}(-Var_p(\mathcal{P}_a)) \tag{17}$$

And thus $\forall a, Var(\mathcal{P}_a) < Var(\mathcal{P}_a^*)$: in each age-class, the variance of parity is lower for the population modeled by $\mathbf{L}$ than for the population modeled by $\mathbf{L}^*$. At a given time, in age class a of each population, some individuals will be removed, their lifetime trajectory stopped and therefore their parity at that time will be the realization of their $\mathcal{LRS}$. As survival is the same for both populations (and here independent from parity), we get $\sigma^2_{\mathcal{LRS}} = \sum_{a=1}^{\omega} Var(\mathcal{P}_a).\prod_{i=1}^{a-1} s(i)$ and therefore we get

$$\sigma^2_{\mathcal{LRS}}(\mathbf{L}) - \sigma^2_{\mathcal{LRS}}(\mathbf{L}^*) = \sum_{a=1}^{\omega}(Var(\mathcal{P}_a) - Var(\mathcal{P}_a^*)).\prod_{i=1}^{a-1} s(i) \le 0 \tag{18}$$

S.5 Effect of *fixed* heterogeneity on $\sigma^2_{\mathcal{LRS}}$

We analyze here the cross-effects of *individual* costs and *fixed* heterogeneity on the variance in reproductive success of the overall population. We try and hint at the relative effects of heterogeneity and individual stochasticity in the making of $\sigma^2_{\mathcal{LRS}}$.

Heterogeneity, costs and $\sigma^2_{\mathcal{LRS}}$

Imagine that the population modeled by $\mathbf{L}$ contains two genotypes. These two genotypes will therefore also be found in $\mathbf{L}^*$ which is an (*age-heterogeneity*) MPPM, corresponding to $\mathbf{L}$ *folded* over *parity*. By the principles of the TLA $\boldsymbol{w^*}$, the (*age-heterogeneity*) right eigenvector, associated to λ for $\mathbf{L}^*$, corresponds to $\boldsymbol{w}$ the (*age-parity-heterogeneity*) right eigenvector of $\mathbf{L}$ when summed on parity. Since offspring are all of parity 0, this implies that the offspring abundances are the same for both models: $\boldsymbol{w^{*\diamond}} = \boldsymbol{w^{\diamond}}$. Put simply, this means that the effects of the *individual* costs and *fixed* heterogeneity are independent. This can be further understood by considering the strategy component of $\sigma^2_{\mathcal{LRS}}$. From the equality between offspring abundances and between $\boldsymbol{\mathcal{R}_0}$(see section S.3) between the two models, we have $\sigma^{\text{fix}}_{\mathcal{LRO}}{}^2(\mathbf{L}) = \sigma^{\text{fix}}_{\mathcal{LRO}}{}^2(\mathbf{L}^*)$, and therefore,

$$\sigma^2_{\mathcal{LRS}}(\mathbf{L}) - \sigma^2_{\mathcal{LRO}}(\mathbf{L}^*) = \sigma^{\text{dyn}}_{\mathcal{LRS}}{}^2(\mathbf{L}) - \sigma^{\text{dyn}}_{\mathcal{LRS}}{}^2(\mathbf{L}^*)$$
$$= w_1^{\diamond}.(\sigma^2_{\mathcal{LRS}_1}(\mathbf{L}) - \sigma^2_{\mathcal{LRS}_1}(\mathbf{L}^*)) + w_2^{\diamond}.(\sigma^2_{\mathcal{LRS}_2}(\mathbf{L}) - \sigma^2_{\mathcal{LRO}_2}(\mathbf{L}^*))$$

is independent from *heterogeneity*.

Order of magnitude of heterogeneity component of $\sigma^2_{\mathcal{LRS}}$

If the difference in variance in $\mathcal{LRS}$ between the models with and without the costs only depends on the stochastic difference – i.e., on the differences at the level of each genotype – the variance itself can be strongly impacted by heterogeneity, and specifically by differences in $\mathbf{R_0}$. As can be shown, the effect of heterogeneity on the variance of $\mathcal{LRS}$ is exactly proportional to both the square of the difference in $\boldsymbol{\mathcal{R}_0}$ and to the variance of the offspring distribution. These two components are not independent (high difference in reproductive rates causes high difference in genotypic λ and therefore large discrepancy in offspring abundances) but for small variations, the heterogeneity component of $\sigma^2_{\mathcal{LRS}}$ is maximal, for two genotypes cohabiting in the population, when $w_1 = w_2 = \frac{1}{2}$ and the difference in $\boldsymbol{\mathcal{R}_0}$ between the genotypes is maximum. This implies that they are located – in the zero-parity vital rate map of Figure 1d – on a line orthogonal to the iso-$\boldsymbol{\mathcal{R}_0}$ curve. For the 5-year models figured in Fig. 1, moving away from a stationary mean genotype located at $(f,s) = (.60, 49)$ in a direction (roughly $(1,1)$) orthogonal to the stationary line, towards coordinates $(f_1, s_1) = (.70, 59)$ on one side and $(f_2, s_2) = (.50, 39)$ on the other side. For the

mean genotype (i.e., for the Reference Leslie matrix of the model) $\mathbf{R_0} \approx 1$, $\lambda \approx 1$, $\sigma^2_{\mathcal{LRS}}(\mathbf{L}) = .594$ (for the full model) $\sigma^2_{\mathcal{LRS}}(\mathbf{L}^*) = .6862$ (for the model folded on *parity*). For the fitter genotype (numbered 1), $\mathbf{R_{01}} = 1.2947$, $\lambda = 1.1986$ $\sigma^2_{\mathcal{LRS}}(\mathbf{L_1}) = .7071$ and $\sigma^2_{\mathcal{LRO}}(\mathbf{L_1^*}) = .8461$, whereas for the frailer genotype (numbered 2), $\mathbf{R_{02}} = 0.7528$, $\lambda = 0.8310$ $\sigma^2_{\mathcal{LRO}}(\mathbf{L_2}) = .4776$ and $\sigma^2_{\mathcal{LRO}}(\mathbf{L_2^*}) = .5293$. For this heterogeneous population, we can therefore compute the *heterogeneity* component of $\sigma^2_{\mathcal{LRS}}$: $\sigma^{\mathrm{fix}}_{\mathcal{LRO}}{}^2 = w_1(1-w_1)*(\mathbf{R_{01}}-\mathbf{R_{02}})^2 = (0.5)^2(1.2947-0.7528)^2 = 0.0734$. And the stochastic component component for the model with the costs $\sigma^{\mathrm{dyn}}_{\mathcal{LRS}}{}^2 = w_1.\sigma^2_{\mathcal{LRS}}(\mathbf{L_1}) + w_2.\sigma^2_{\mathcal{LRO}}(\mathbf{L_2}) = 0.5 \times 0.7071 + 0.5.4776 = 0.5923$ and without the costs $\sigma^*_{\mathcal{LRS}}{}^{\mathrm{sto}^2} = w_1.\sigma^2_{\mathcal{LRS}}(\mathbf{L_1^*}) + w_2.\sigma^2_{\mathcal{LRO}}(\mathbf{L*_2}) = 0.5 \times 0.8461 + 0.5.5293 = 0.6877$. We can see here, that even though the costs raise the heterogeneity component of $\sigma^2_{\mathcal{LRS}}$ in the population from $\frac{0.0734}{0.6862} = 0.107$ to $\frac{0.0734}{0.594} = 0.123$ (as they keep the heterogeneity component unchanged), that the demographic variance of a population is more driven by stochasticity than heterogeneity, even for genotypes with differences in fitness.